2D compressibility of surface states on 3D topological insulators

D. S. L. Abergel and S. Das Sarma
Condensed Matter Theory Center, University of Maryland, College Park, Maryland 20742, USA

We develop a theory for the compressibility of the surface states of 3D topological insulators and propose that surface probes of the compressibility via scanning single electron transistor microscopy will be a straightforward way to access the topological states without interference from the bulk states. We describe the single-particle nature of the surface states taking into account an accurate Hamiltonian for the bands and then include the contribution from electron–electron interactions and discuss the implications of the ultra-violet cutoff, including the universality of the exchange contribution when expressed in dimensionless units. We also compare the theory with experimentally obtained $\frac{d\mu}{dn}$ as extracted from angle-resolved photoemission spectroscopy measurements. Finally, we point out that interaction-driven renormalization of the Fermi velocity may be discernible via this technique.

Recently, there has been great interest in trying to engineer materials with topologically protected states because of the applications that such states may find in quantum computing. In particular, it was predicted that certain 3D layered crystals with strong spin-orbit coupling and an inverted conduction band would have an insulating band gap in the bulk, but topologically robust conducting surface states with linear low-energy dispersion protected by time-reversal symmetry.[1] Angle-resolved photo-emission spectroscopy (ARPES) experiments on crystals such as Bi_2Te_3 and Bi_2Se_3 have proven the existence of these mid-gap surface states with nearly linear spectra.[2–5] However, in most current samples the Fermi energy is well above the bulk gap meaning that transport measurements of the surface states are difficult because current can also flow in the bulk of the crystal[6], *i.e.* the bulk is a conductor rather than an insulator even at low temperature[7], although this can be mitigated to some extent by using thin films of the topological insulator (TI) crystal[8] or by doping the crystal to compensate for the bulk conduction.[9] Therefore, it is essential that methods are found to both control and characterize these topologically protected states.

In this Rapid Communication, we propose using single electron transistor (SET) microscopy[10,11] as a way of mitigating the effect of the bulk states by approaching the surface directly. Local capacitance measurements made via this technique can be converted straightforwardly into the quantity $\frac{d\mu}{dn}$ (where μ is the chemical potential and n is the carrier density in the surface state) which is directly linked to the band structure and to the electronic compressibility. A great advantage of measuring this thermodynamic compressibility is that it incorporates single-particle many-body renormalization directly,[12] and thus, quantitative information both about the single-particle (SP) band structure and many-body renormalization are obtained in one stroke as a function of 2D carrier density (or equivalently, the 2D Fermi energy of the surface states). We begin by calculating $\frac{d\mu}{dn}$ for two different commonly used approximations for the noninteracting band structure of the Hamiltonian for the surface states of TIs such as Bi_2Se_3 and Bi_2Te_3 and then take into account the electron-electron interaction demonstrating that this contribution is universal and identical for both band structure approximations when expressed in dimensionless units. However, we demonstrate that the high dielectric constant of these materials reduces the quantitative effect of the interactions. We also argue that it may be possible to observe renormalization of the quasiparticle Fermi velocity at sufficiently low density by this technique. We then compare the results of our analytical SP calculations to estimations of $\frac{d\mu}{dn}$ extracted from ARPES measurements of the band structure. Finally, we comment on the role of disorder and charge inhomogeneity on $\frac{d\mu}{dn}$ in these systems.

If the plane of the surface corresponds to the (111) crystal direction (*i.e.* parallel to the layered structure of the lattice) then the simplest approximation for the band structure is the commonly-used linear approximation given by the Hamiltonian[1] $H^l = \hbar v_F \sigma \cdot \mathbf{k}$ where v_F is the band velocity, $\mathbf{k}$ is the two-dimensional wave vector in the plane of the surface, and $\sigma_{x,y}$ are Pauli matrices in the real spin space. The spectrum of this Hamiltonian is trivially the linear Dirac dispersion given by $\varepsilon^l_{\lambda k} = \lambda \hbar v_F k$ where $\lambda = \pm 1$ denotes the band. The corresponding eigenvectors are two-component spinors in the spin space. The 2D density of carriers in the SP limit is given by $n = k_F^2/(4\pi)$ where k_F is the Fermi wave vector and as a matter of convention, we say that zero density corresponds to the chemical potential being located at the Dirac point. Elementary manipulations show that

$$\frac{d\mu}{dn} = \hbar v_F \sqrt{\frac{\pi}{|n|}} \tag{1}$$

A more sophisticated approximation for the band Hamiltonian including the curvature in the valence band which is noticeable in the ARPES data is $H^q = \frac{\hbar^2 k^2}{2m^*} + \hbar v_F \sigma \cdot \mathbf{k}$ where m^* is the effective mass of the carriers.[13] The spectrum associated with this Hamiltonian is $\varepsilon^q_{\lambda k} = \frac{\hbar^2 k^2}{2m^*} + \lambda \hbar v_F k$. These spectra are shown in Fig. 1(a). In the case with the quadratic correction, there is an unphysical turning point in the valence band which demands that some care must be taken when describing this band. The turning point is located at at $k_0 = v_F m^*/\hbar$,

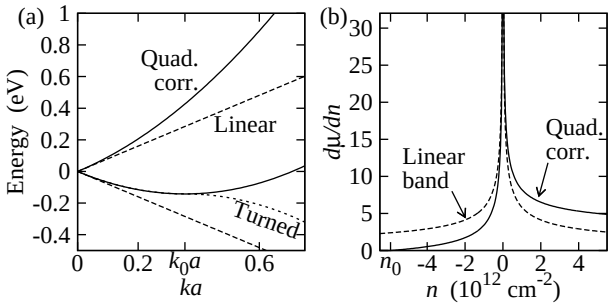

FIG. 1. (a) Single particle bands. The dotted line is the 'turned' band structure where the quadratic band is inflected at its turning point. (b) Single particle $\frac{d\mu}{dn}$ corresponding to Eqs. (1) and (2).

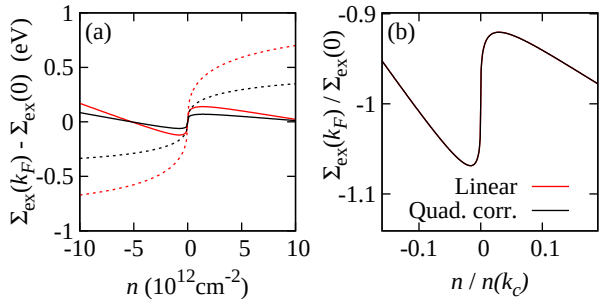

FIG. 2. (a) The self-energy relative to its value at zero density. Solid lines indicate $k_c = 1/a$ and dashed lines show $k_c = 2\pi/a$. (b) The self-energy normalized by its absolute value at zero density. Lines for both dispersions and all values of k_c collapse onto each other. Throughout, the linear band is shown by red lines and the quadratic band by black lines.

the energy at this wave vector is $\varepsilon_0 = -\frac{v_F^2 m^*}{2}$, and the associated density is $n_0 = -m^{*2} v_F^2/(4\pi\hbar^2)$. Hence, defining wave vectors, energies, or densities which are greater in magnitude than k_0, ϵ_0, and n_0 requires a specific definition of the band structure, and this will become vital when the interaction effects are incorporated. We defer further discussion of this specific point until it is relevant. However, for $n > n_0$ we use the relationship for the density above, and find

$$\frac{d\mu}{dn} = \frac{2\pi \mathrm{sgn}(n)\hbar^2}{m^*} + \hbar v_F \sqrt{\frac{\pi}{|n|}} \qquad (2)$$

where $\mathrm{sgn}(x)$ denotes the sign of the argument. Figure 1(b) shows the single-particle $\frac{d\mu}{dn}$ for each approximation as a function of density. Unless otherwise stated, we use $v_F = 5\times10^5 \mathrm{ms}^{-1}$, $m^* = 0.2 m_e$ (m_e is the electron mass), and $a = 0.41\mathrm{nm}$ throughout this paper. The quadratic correction preserves the dominant $1/\sqrt{n}$ behavior at low density, but introduces an asymmetry between the conduction and valence bands. In addition, $\frac{d\mu}{dn}$ goes to zero at n_0.

We now include the effect of the electron–electron interaction on the compressibility. Evaluating the self-energy contribution from the exchange interaction gives

$$\Sigma_{\mathrm{ex},\lambda}(\mathbf{k}) = -\frac{1}{8\pi^2}\int d^2\mathbf{q} \sum_{\lambda'} V_C(\mathbf{q}) f_{\lambda'}(\mathbf{k}+\mathbf{q}) \times \times \left[1 + \lambda\lambda' \cos(\theta_{k+q} - \theta_k)\right] \qquad (3)$$

where $V_C(\mathbf{q}) = 2\pi e^2/(\kappa|\mathbf{q}|)$ is the two-dimensional Fourier-transformed unscreened Coulomb interaction, κ is the static dielectric constant of the environment, $f_\lambda(\mathbf{k})$ is the occupancy of the state with wave vector $\mathbf{k}$ in band λ, θ_k is the angle that the wave vector $\mathbf{k}$ makes with the x axis. It is well-known that for the compressibility the exchange energy (or equivalently, the Hartree-Fock term) is the dominant interaction correction, and this is even more true for TI systems because of their very large background dielectric constant. Therefore we anticipate very small interaction corrections beyond exchange in this problem. Note that the only place that the band structure enters into this expression is in the occupancy factors so that it is applicable to systems described by both H^l and H^q. At zero temperature the angular part of the integration of $\mathbf{q}$ can be computed analytically and yields

$$\Sigma_{\mathrm{ex},\lambda}(\mathbf{k}) = -\frac{e^2}{4\pi\kappa}\int_0^{k_c} dk' \sum_{\lambda'} Y_{\lambda k \lambda' k'} \Theta\left(\mu - \varepsilon_{\lambda' k'}\right)$$

where the appropriate SP energy must be inserted into the step function,

$$Y_{\lambda k \lambda' k'} = \frac{2}{k}\begin{cases} (k'+k)\left[K(X) - E(X)\right] & \lambda\lambda' = 1 \\ \frac{(k'-k)^2}{k'+k}K(X) - (k'+k)E(X) & \lambda\lambda' = -1 \end{cases},$$

K and E are complete elliptic integrals of the first and second kind, and $X = 2\sqrt{kk'}/(k+k')$. The radial integral must be evaluated numerically. We note that the exchange integral of Eq. (3) has an ultraviolet high momentum divergence arising from the linear dispersion, which must be regularized through a high wave vector cut off k_c. As is usual in condensed matter physics, there is a real cut off in the momentum arising from the lattice structure, and therefore, $k_c \sim 1/a$, and the interaction strength depends explicitly on the short-distance lattice cut-off in the theory. To illustrate the qualitative features of the physics, and to determine the dependence of $\frac{d\mu}{dn}$ on k_c we start by describing the $\kappa = 1$ case in which interactions are the strongest. This function is shown in Fig. 2(a) for both the linear band and the band with a quadratic correction for two different values of the ultraviolet cutoff. Details of the definition of the band structure for the quadratic correction are given below. In Fig. 2(b), the same data is shown but the units are scaled to demonstrate how the self-energy depends on the cutoff k_c. The linear and quadratic bands give identical results when the self-energy is scaled by its value at zero density. We emphasize that this result shows the universality of the exchange contribution, which is reminiscent of similar results found in semiconductor heterostructures.[14,15]

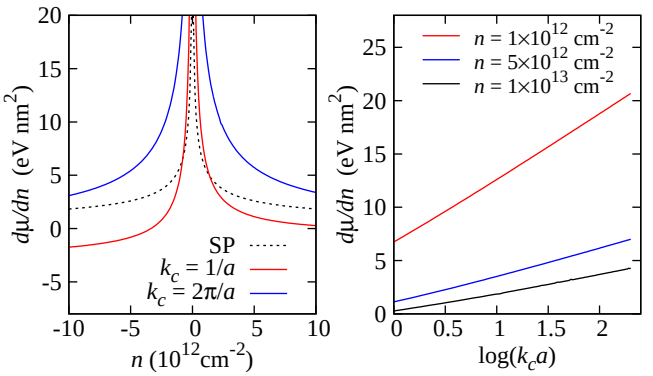

FIG. 3. Linear band. (a) $\frac{d\mu}{dn}$ as a function of density for the single-particle band, and two values of k_c. This illustrates that the choice of k_c is crucial: small k_c gives a negative contribution to $\frac{d\mu}{dn}$ at higher densities, large k_c gives a positive contribution. (b) $\frac{d\mu}{dn}$ as a function of $\log(k_c a)$ for different carrier densities.

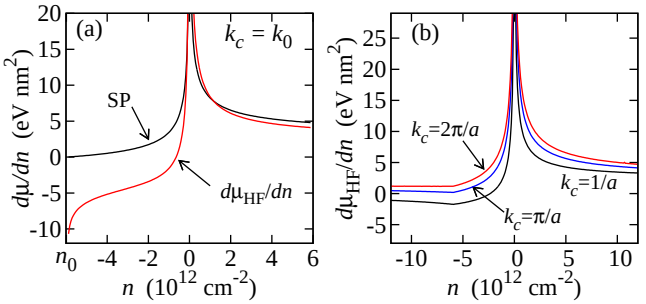

FIG. 4. The quadratic correction. (a) $\frac{d\mu}{dn}$ for $k_c = k_0$. (b) $\frac{d\mu}{dn}$ for various values of $k_c > k_0$.

The independence of the dimensionless many-body corrections of the details of the TI band structure is an important new result of our work.

The exchange self-energy is incorporated into the calculation for $\frac{d\mu}{dn}$ in the following way. The Hartree-Fock chemical potential is the sum of the SP kinetic energy and the exchange self-energy: $\mu_{\rm HF} = \mu + \Sigma_{\rm ex}$ and the corresponding compressibility is given by $d\mu_{\rm HF}/dn$, which may be computed numerically. When applied to the linear band structure associated with H^l, the expression in Eq. (3) contains an ultra-violet divergence and so the value of the high-frequency cutoff k_c becomes important, as hinted at in Fig. 2. In Fig. 3(a) we show $\frac{d\mu}{dn}$ for the linear band with the exchange contribution for two different physically reasonable values of k_c. In all cases, the $n^{-\frac{1}{2}}$ behavior persists at low density. For $k_c = 1/a$ the exchange causes a reduction in $\frac{d\mu}{dn}$ relative to the SP case for all but the lowest densities and may become negative for large valence band doping. In contrast, $k_c = 2\pi/a$ gives an enhancement to $\frac{d\mu}{dn}$. This indicates that the precise value of the ultraviolet k_c has an important quantitative effect on $\frac{d\mu}{dn}$. In Fig. 3(b) we show the dependence of $\frac{d\mu}{dn}$ on k_c for three different values of the density. Noting the logarithmic scale on the k_c axis, we see that $\frac{d\mu}{dn} \propto \log(k_c a)$. Hence, in order to make quantitative predictions of the behavior of $\frac{d\mu}{dn}$ at finite density, some physical intuition must be used for choosing the 'correct' value of k_c. On the other hand, the logarithmic dependence of the interaction effect on $k_c a$ translates basically into a slow logarithmic renormalization of the coupling strength in units of k_c/k_F which could manifest itself at very low carrier densities.[16]

For the quadratic band, Eq. (3) still holds, but the appropriate dispersion must be used in the Fermi function. The shape of the valence band introduces a further complication. Taken at face value, the band minimum at k_0 should be interpreted as producing a Fermi surface with non-trivial topology, and contributions to $\frac{d\mu}{dn}$ should be included from both branches of the valence band. However, this does not correspond to the experimental data (see, for example, Ref. 17) where the turning point is not seen. The first (and most intuitive choice) is to set $k_c = k_0$. This may be physically reasonable because the topological surface bands typically merge with the bulk bands at roughly this wave vector. Another possibility is to artificially turn the band structure for $|k| > k_0$ in the valence band (as illustrated by the dotted line in Fig. 1(a)) so that for $|k| > k_0$ we have $\varepsilon^q_{-k} = -\frac{\hbar^2 k^2}{2m^*} - \hbar v_F k$. Then, from a technical point of view, k_c can be set arbitrarily high and the quadratically-dispersing nature of the band is retained. Figure 4(a) shows the first of these cases. Since k_c is relatively small, the density can reach the regime where the self-energy is decreasing rapidly, $n/n(k_c) \sim 0.1$. In that case, the negative slope of the exchange energy is stronger than the positive slope of the SP chemical potential so that $\mu_{\rm HFA}$ is a decreasing function of n for $n < 0$ implying that $d\mu_{\rm HFA}/dn$ is negative. We believe that some of these interesting questions about the precise value of the ultraviolet cut-off in this problem can actually be answered through a careful comparison between experiment and theory on the TI compressibility.

For the turned band structure with $k_c > k_0$, the evolution of $\Sigma_{\rm ex}$ with increasing k_c means that the sign of the exchange contribution can be positive or negative. For a given density, we have $\frac{d\mu}{dn} \propto \log(k_c a)$ as was the case for the linear band.

The static dielectric constant of crystals such as Bi_2Se_3 and Bi_2Te_3 is estimated to be[7,18] greater than 50 which will naturally have the effect of reducing the strength of the interactions. If we assume that the effective dielectric constant is the average of that in the material and that of the air then we can take a physically reasonable value of $\kappa = 20$. Figure 5 shows that the exchange contribution to $\frac{d\mu}{dn}$ is reduced so much that it is essentially non-existent. Hence, for the purposes of examining the compressibility of the surface states, the SP calculation is likely to be quantitatively sufficient.

At this point, we pause to comment on another experimental manifestation of the exchange self-energy. In

principle, the Fermi velocity is renormalized by this interaction[19,20] and there has been some experimental hint of this in graphene in both zero magnetic field[21] and high magnetic fields.[22–24] The renormalized quasiparticle velocity can be written as

$$v_{F,\mathrm{int}} = \frac{1}{\hbar}\frac{d\mu_{\mathrm{HF}}}{dk} \sim \left(1 + r_s \log\frac{k_c}{k_F}\right)$$

with $r_s = e^2/(\hbar\kappa v_F)$ and thus the interaction-induced correction will be proportional to $\log(k_c/k_F)$. Of course, the Fermi velocity measured in experiment includes this renormalization so it is not directly measurable, but since the self-energy is a non-monotonic function of the wave vector, its effect may be seen by a density-dependent deviation of the Fermi velocity from a constant value which represents the combination of the SP and mean interaction contributions. Such a nonlinear reconstruction of the 2D TI Fermi surface at low carrier density will be a direct manifestation of its Dirac spectrum and the associated ultraviolet renormalization effect familiar in quantum electrodynamics.

We can also extract $\frac{d\mu}{dn}$ from ARPES measurements of the band structure. Digitizing curves from Zhu *et al.*[5] gives the band structure of Bi_2Se_3 in the $K\Gamma K$ direction from which we can numerically extract $\frac{d\mu}{dn}$ for comparison to theory. However, this process is complicated by the fact that the curves on either side of the Γ point are not perfectly symmetric, it is also known that there is a hexagonal distortion to the Fermi surface,[2] and ARPES data contains some noise. To combat these difficulties we apply a Gaussian smoothing convolution to the experimental data with a width $\sigma = 0.08\mathrm{nm}^{-1}$ to both branches shown in the $K\Gamma K$ plot and take the average of the two to arrive at the approximate band structure. Then we associate the Fermi wave vector k_F with this averaged curve for each value of energy and from this compute the density as $n = k_F^2/(4\pi)$ which assumes a circular Fermi surface. A numerical derivative of the chemical potential with respect to the density may then be taken. The results of this procedure are shown in Fig. 5(b) along with a least-squares best fit of the quadratic correction dispersion using m^* and v_F as fitting parameters from the conduction band data. This fitting procedure yielded $m^* = 0.417m_e$ and $v_F = 1.00 \times 10^6\mathrm{ms}^{-1}$, both of which are larger than the current common estimates for these parameters in Bi_2Se_3. The dashed line corresponds to the predicted $\frac{d\mu}{dn}$ for a purely quadratic band, which is constant at a value of $\frac{d\mu}{dn} = \frac{2\pi\hbar^2}{m^*} \approx 1.15\mathrm{eVnm}^2$. This indicates that the quadratic part of the band is completely dominated by the linearity of the band structure over the whole experimentally pertinent range of carrier density very clearly establishing that the Dirac spectrum is dominating the physics in these systems.

One likely challenge to using the compressibility to investigate the topological surface states is the observed existence of substantial disorder-induced inhomogeneity in the charge landscape of the surface.[25] Surface probes

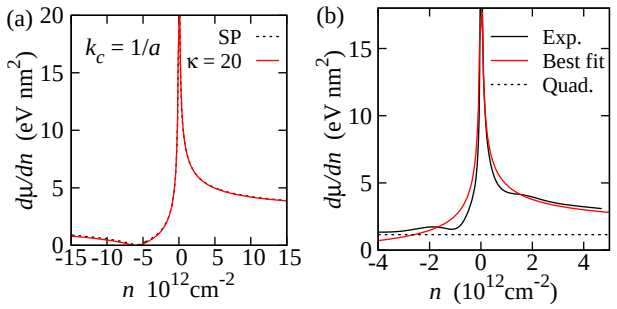

FIG. 5. (a) The effect of electron-electron interactions for the quadratic band with $\kappa = 20$ and $k_c = 1/a$. (b) Black line: $\frac{d\mu}{dn}$ computed from band structure extracted from ARPES data in Zhu *et al.*[5] (see text for details). Red line: least-squares best fit to the analytical result of Eq. (2). The parameters extracted from the conduction band are $m^* = 0.417m_e$ and $v_F = 1.00 \times 10^6\mathrm{ms}^{-1}$.

such as scanning tunneling microscopy have shown that the screening of an external disorder potential created by charged impurities in the lattice of Bi_2Te_3 and Bi_2Se_3 lead to the formation of 'puddles' of electron and holes with spatial extent of the order of 10nm and associated fluctuations in the local chemical potential of approximately 10meV. This fluctuation has previously been investigated in the context of charge transport,[26] but in the case of our proposed SET measurements, it should be pointed out that the area of the sample which influences the tip has a radius[10,11] of the order of 100nm, much larger than one puddle. Therefore, the SET will experience some averaged field corresponding to the inhomogeneous landscape. The effect of the inhomogeneity is that even when the global average of the density is zero, the local density is always finite and may be positive or negative. Therefore, in the inhomogenous case, the local density never approaches zero and hence the $1/\sqrt{n}$ divergence is curtailed. At high density, the slow change of $\frac{d\mu}{dn}$ with density implies that the inhomogeneity will have little effect on the measured compressibility. Therefore, the extraction of band parameters from SET data is likely to be most accurate at higher density.

In this Rapid Communication, we have proposed that a capacitive surface probe such as SET microscopy will reveal the properties of the topological surface states of crystals such as Bi_2Te_3 and Bi_2Se_3 via measurement of the compressibility, or $\frac{d\mu}{dn}$. We have analytically computed the SP contribution to $\frac{d\mu}{dn}$ for two different model band structures and described the role that electron-electron interactions and charge inhomogeneity in the crystal will play. In summary, the high dielectric constant implies that the quantitative effect of interactions is negligable (although at low density there is some hope of detecting a renormalization of the Fermi velocity due to electron-electron interactions), and the inhomogeneity can be accounted for via a straightforward phenomenological averaging technique which will result in the low-density divergence being cut off. We have established

that compressibility measurements, when compared with theory, could provide valuable information about both SP and many-body properties of 2D TI surface states.

We thank US-ONR for support.

[1] H. Zhang, C.-X. Liu, X.-L. Qi, X. Dai, Z. Fang, and S.-C. Zhang, Nat Phys **5**, 438 (2009).

[2] Y. L. Chen, J. G. Analytis, J.-H. Chu, Z. K. Liu, S.-K. Mo, X. L. Qi, H. J. Zhang, D. H. Lu, X. Dai, Z. Fang, S. C. Zhang, I. R. Fisher, Z. Hussain, and Z.-X. Shen, Science **325**, 178 (2009).

[3] Y. Zhang, K. He, C.-Z. Chang, C.-L. Song, L.-L. Wang, X. Chen, J.-F. Jia, Z. Fang, X. Dai, W.-Y. Shan, S.-Q. Shen, Q. Niu, X.-L. Qi, S.-C. Zhang, X.-C. Ma, and Q.-K. Xue, Nat Phys **6**, 584 (2010).

[4] Y. Xia, D. Qian, D. Hsieh, L. Wray, A. Pal, H. Lin, A. Bansil, D. Grauer, Y. S. Hor, R. J. Cava, and M. Z. Hasan, Nat Phys **5**, 398 (2009).

[5] Z.-H. Zhu, G. Levy, B. Ludbrook, C. N. Veenstra, J. A. Rosen, R. Comin, D. Wong, P. Dosanjh, A. Ubaldini, P. Syers, N. P. Butch, J. Paglione, I. S. Elfimov, and A. Damascelli, Phys. Rev. Lett. **107**, 186405 (2011).

[6] H. Steinberg, D. R. Gardner, Y. S. Lee, and P. Jarillo-Herrero, Nano Lett. **10**, 5032 (2010).

[7] N. P. Butch, K. Kirshenbaum, P. Syers, A. B. Sushkov, G. S. Jenkins, H. D. Drew, and J. Paglione, Phys. Rev. B **81**, 241301 (2010).

[8] D. Kim, S. Cho, N. P. Butch, P. Syers, K. Kirshenbaum, S. Adam, J. Paglione, and M. S. Fuhrer, Nat. Phys. **8**, 460 (2012).

[9] Z. Ren, A. A. Taskin, S. Sasaki, K. Segawa, and Y. Ando, Phys. Rev. B **85**, 155301 (2012).

[10] M. J. Yoo, T. A. Fulton, H. F. Hess, R. L. Willett, L. N. Dunkleberger, R. J. Chichester, L. N. Pfeiffer, and K. W. West, Science **276**, 579 (1997).

[11] A. Yacoby, H. Hess, T. Fulton, L. Pfeiffer, and K. West, Solid State Communications **111**, 1 (1999).

[12] Q. Li, E. H. Hwang, and S. Das Sarma, Phys. Rev. B **84**, 235407 (2011).

[13] D. Culcer, E. H. Hwang, T. D. Stanescu, and S. Das Sarma, Phys. Rev. B **82**, 155457 (2010).

[14] S. Das Sarma, R. Jalabert, and S.-R. E. Yang, Phys. Rev. B **41**, 8288 (1990).

[15] E. H. Hwang and S. Das Sarma, Phys. Rev. B **58**, R1738 (1998).

[16] Note that in graphene, the cut-off may be set by stipulating that number of states in each band corresponds to one electron per atom but no such reasoning exists for TI crystals.

[17] M. Z. Hasan and C. L. Kane, Rev. Mod. Phys. **82**, 3045 (2010).

[18] W. Richter and C. R. Becker, physica status solidi (b) **84**, 619 (1977).

[19] E. H. Hwang, B. Y.-K. Hu, and S. Das Sarma, Phys. Rev. Lett. **99**, 226801 (2007).

[20] S. Das Sarma and E. H. Hwang, ArXiv e-prints (2012), arXiv:1203.2627 [cond-mat.mes-hall].

[21] D. C. Elias, R. V. Gorbachev, A. S. Mayorov, S. V. Morozov, A. A. Zhukov, P. Blake, L. A. Ponomarenko, I. V. Grigorieva, K. S. Novoselov, F. Guinea, and A. K. Geim, Nat Phys **7**, 701 (2011).

[22] Z. Jiang, E. A. Henriksen, L. C. Tung, Y.-J. Wang, M. E. Schwartz, M. Y. Han, P. Kim, and H. L. Stormer, Phys. Rev. Lett. **98**, 197403 (2007).

[23] G. Li, A. Luican, and E. Y. Andrei, Phys. Rev. Lett. **102**, 176804 (2009).

[24] S. Y. Zhou, G.-H. Gweon, J. Graf, A. V. Fedorov, C. D. Spataru, R. D. Diehl, Y. Kopelevich, D.-H. Lee, S. G. Louie, and A. Lanzara, Nat Phys **2**, 595 (2006).

[25] H. Beidenkopf, P. Roushan, J. Seo, L. Gorman, I. Drozdov, Y. S. Hor, R. J. Cava, and A. Yazdani, Nat Phys **7**, 939 (2011).

[26] S. Adam, E. H. Hwang, and S. Das Sarma, Phys. Rev. B **85**, 235413 (2012).